Detection of atomic oxygen in a plasma-assisted flame via a backward lasing technique

Ding, Pengji; Ruchkina, Maria; Del Cont-Bernard, Davide; Ehn, Andreas; Lacoste, Deanna A.; Bood, Joakim

Published in:
Optics Letters

DOI:
10.1364/OL.44.005477

2019

Document Version:
Peer reviewed version (aka post-print)

Citation for published version (APA):
Ding, P., Ruchkina, M., Del Cont-Bernard, D., Ehn, A., Lacoste, D. A., & Bood, J. (2019). Detection of atomic oxygen in a plasma-assisted flame via a backward lasing technique. *Optics Letters*, *44*(22), 5477-5480. https://doi.org/10.1364/OL.44.005477

Total number of authors:
6

Detection of atomic oxygen in a plasma-assisted flame via a backward lasing technique

Pengji Ding[1], Maria Ruchkina[1], Davide Del Cont-Bernard[2], Andreas Ehn[1], Deanna A. Lacoste[2], and Joakim Bood[1]

1. Division of Combustion Physics, Department of Physics, Lund University, Box 118, 221 00 Lund, Sweden
2. Clean Combustion Research Center, King Abdullah University of Science and Technology, Thuwal, 23955-6900, Saudi Arabia

Abstract

In this Letter, we have investigated 845 nm lasing generation in atomic oxygen, present in a lean methane-air flame, using two-photon pumping with femtosecond 226 nm laser pulses, particularly focusing on the impact of nanosecond repetitively pulsed glow discharges forcing on the backward lasing signal. Characterizations of the backward lasing pulse, in terms of its spectrum, beam profile, pump pulse energy dependence, and divergence, were conducted to establish the presence of lasing. With plasma forcing of the flame, the backward lasing signal was observed to be enhanced significantly, ~50%. The vertical concentration profile of atomic oxygen was revealed by measuring the backward lasing signal strength as a function of height in the flame. The results are qualitatively consistent with results obtained with two-dimensional femtosecond two-photon absorption laser-induced fluorescence, suggesting that the backward lasing technique can be a useful tool for studies of plasma-assisted combustion processes, particularly in geometries requiring single-ended standoff detection.

By focusing a pump laser onto a tiny volume of atoms or molecules, highly directional emission or "lasing" along the pump laser beam, in both the forward and backward directions, may emerge at a wavelength different from that of the pump laser. Backward lasing travels back towards the pump laser and, thus, samples the intervening medium as it returns. As such, backward lasing could potentially provide single-ended remote sensing of atomic/molecular species that are difficult or impossible to study with conventional laser-based techniques. It could be used to monitor atmospheric pollutants, trace gases remaining indicative of hazardous substances, such as explosive devices, or investigate combustion conditions in furnaces and engines, just to give a few examples. Driven by its very promising potential to manage the aforementioned applications, backward lasing techniques have lately been a topic of intense research within the research communities of ultrafast optics and laser-based diagnostics. The pioneering works on backward lasing in air by Luo et al. [1] and Dogariu et al. [2] have been followed by a significant number of papers demonstrating various measurement concepts and applications; see, e.g., Refs. [3–10].

These vivid activities were inspired by earlier works in flames, in which backward lasing of important intermediate species, such as O, H, and C atoms, have been observed with nanosecond (ns) laser pumping [11–13]. However, the observed backward lasing pulses had a ns-scale duration with spiky temporal profiles, resulting in poor and ambiguous spatial resolution, severely limiting its diagnostic potential. In addition, the high UV-pulse energy required for efficient pumping, typically a few millijoules, makes the concept prone to photolytic interferences. To overcome these difficulties, we recently demonstrated backward lasing from atomic hydrogen in flames based on femtosecond (fs) laser pumping, which produced backward lasing pulses of picosecond-scale duration and with smooth temporal profiles [14,15]. These characteristics of the lasing pulses, together with high time-resolved detection, allow single-ended measurements with spatial resolution on the millimeter scale for the backward lasing technique (BLT). The potential of the method for combustion diagnostics has recently been demonstrated in laboratory flames, where it was shown that the hydrogen signal from two reaction zones separated by 2 mm can be resolved and that the lasing signal is strong enough for single-shot measurements [14,16].

In this Letter, we apply the BLT to assess the impact of plasma induced by nanosecond repetitively pulsed (NRP) glow discharge on a flame in terms of the distribution of atomic oxygen, and compare the results with the corresponding results obtained with femtosecond two-photon-absorption laser-induced fluorescence (fs-TALIF). The oxygen atom was chosen to be studied since it plays an important role in the kinetics of hydrocarbon oxidation, which also makes it a key species and, hence, the interest of plasma-assisted combustion (PAC) applications [17]. For detection of O atoms, two-photon resonant excitation from the 2p3P ground state to the $3p^3P$ excited state is carried out using 226 nm fs laser pulses. De-excitation then takes place from the $3p^3P$ to the $3s^3S$ state, corresponding to a photon wavelength of 845 nm [see Fig. 1(a)]. In addition to relaxation through spontaneous emission, i.e., fluorescence, the highly intense pumping achieved with fs laser pulses can create population inversion between the two states, generating stimulated emission, here referred to as lasing, which was originally observed in sub-atmospheric flames by Aldén et al. [11]. Characterization of the backward lasing pulses from O atoms, including the emission spectrum, spatial profile, and divergence, was first performed to confirm the occurrence of lasing. It was found that the backward lasing signal increased significantly (~54%) with 10 kHz, 8.5 kV glow discharge forcing on the flame. A comparison with two-dimensional (2D) fs-TALIF imaging shows that both techniques can provide reliable vertical profiles of O atoms along the discharge path.

The experimental setup is shown in Fig. 1(b). A wavelength-tunable fs laser system was used to provide 125 fs laser pulses at 226 nm wavelength with a maximum pulse energy of ~200 μJ. The beam size is about 5 mm in diameter, and the spectral bandwidth is about 2 nm (full width at half-maximum). The 226 nm laser beam is first sent through a dispersive prism and then focused with an f = 300 mm spherical CaF2 lens into a V-shaped flame, where atomic oxygen is naturally present. The flame is a lean methane-air flame, confined by a co-flow of nitrogen. It stabilizes between the nozzle and a stagnation quartz plate in a PAC burner (see Fig. 3.8 in Ref. [18]). The equivalence ratio is fixed at 0.76 (i.e., a fuel-lean flame). Two pin electrodes (9 mm gap) are placed in such a way that the pinto-pin glow discharge passes through the symmetry axis of the flame. The inset photos in Figs. 1(c) and 1(d) show direct imaging of the flame without and with NRP glow discharge forcing, respectively. The discharges are produced by high-voltage pulses of 10 ns duration, with an 8.0 kV amplitude between the pin anode in the burner and the grounded pin electrode of the quartz plate, applied at a repetition rate of 10 kHz.

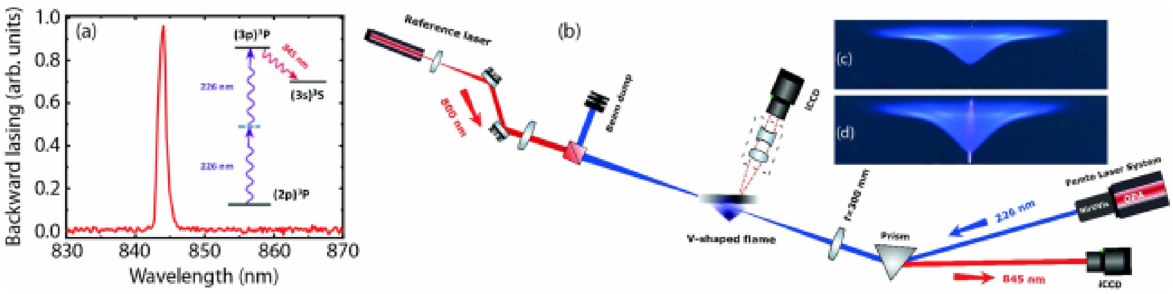

Fig. 1 *(a) Spectrum of 845 nm lasing emission in the backward direction measured with a low-resolution spectrometer. The inset shows the two-photon resonant excitation scheme of the O atom and subsequent emission at 845 nm. (b) Schematic illustration of the experimental setup. Insets (c) and (d) show the side view of the flame without and with plasma forcing produced with 10 kHz, 8.0 kV glow discharge, respectively. The photos were taken with an ordinary digital camera.*

The focusing of 226 nm laser pulses into the flame creates a narrow filamentary excitation volume of O atoms, from which 845 nm lasing occurs in both the forward and backward directions. The backward lasing beam is collimated by the focusing lens and then separated from the incident 226 nm laser beam by a prism. Finally, the backward lasing signal is detected by an intensified CCD camera (iCCD, Princeton Instruments, PI-MAX4 1024f) or a fiber spectrometer [not shown in Fig. 1(b)]. A reference laser beam at 800 nm was used for alignment of the setup, particularly to roughly predict the optical path of the 845 nm backward lasing beam. For 2D fs-TALIF measurements, a ∼5 mm wide laser sheet was created with a cylindrical lens (f = 500 mm) and focused into the flame. The iCCD camera, equipped with a 135 mm f/2.8 lens (Nikon) and two bandpass interference filters, was used to record the fluorescence images of atomic oxygen in the side direction. The camera gate width was 4 ns, and each fs-TALIF image is an accumulation of 250 shots.

We started the experiments in the unperturbed flame, i.e., without plasma forcing. To establish the presence of lasing, the signal emitted backwards along the excitation volume is compared to the fluorescence signal detected from the side direction. Figure 2(a) shows both the backward emission and the fluorescence signal as a function of the 226 nm pump laser pulse energy. If the backward emission is incoherent fluorescence, then these two measurements should give similar scaling behavior. On the other hand, if the backward emission indeed is lasing due to stimulated emission, then the shapes of the curves will be different since lasing requires pump pulse energies above a certain threshold to occur. As can be seen in Fig. 2(a), the fluorescence signal intensity increases gradually with pump pulse energy. Power function fitting to the data suggests a power index of 1.8 0.3, which is consistent with the two-photon process. On the other hand, the backward emission intensity follows a much faster pulse energy dependence, showing clearly different low-pump-intensity behavior from that of the fluorescence signal, which is similar to what has been reported in Refs. [2,11]. The dependence curve also shows the signature of a threshold at ∼45 μJ.

At a position of ∼1.5 m away from the PAC burner, the iCCD camera is used to capture the profile of the backward 845 nm lasing beam. The divergence of the backward lasing beam is determined by measuring its size at two different positions along the propagation path. It is found that backward lasing is very localized with a small beam divergence, another indicative signature of the lasing effect. A typical result, displayed in Fig. 2(b), shows a Gaussian-shaped spatial profile with a divergence of ∼5 mrad. However, it should be noticed that the spatial mode is dynamic, mostly due to pulse-to-pulse energy variations of the 226 nm pump laser. With a relatively stable pump pulse energy of 108.0 ± 5.3 μJ, the divergence of the backward lasing beam is recorded continuously over 100 laser pulses, and the results are shown in Fig. 2(c). The mean divergence is found to be 4.7 mrad with a standard deviation of 0.7 mrad.

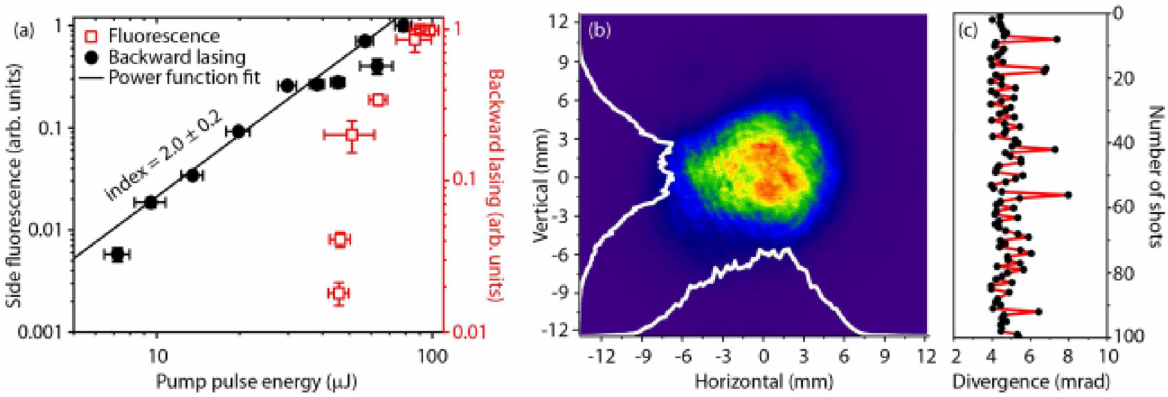

Fig. 2 *(a) Pump pulse energy dependence of the fluorescence signal and backward lasing signals at 845 nm. (b) Far-field, single-shot backward 845 nm lasing beam measured 1.5 m away from the 226 nm laser focusing point in the flame. The white solid lines depict the horizontal and vertical beam profiles. (c) Variation of the lasing beam divergence over 100 laser shots.*

Figure 3 shows the beam divergence of the backward lasing pulse measured at different vertical positions y in the flame. The y = 0 is defined as the position of the upper electrode, and the positive y points to the lower electrode. For y < 2.0 mm, the 226 nm pump laser is blocked by the quartz plate. Below the flame tip where y = 6 mm, there is no detectable lasing signal since there are no O atoms in the cold gases. One can see that the divergence of the backward lasing beam gradually increases with y. Backward lasing beam images recorded at three different vertical positions (3, 4.5, and 6.0 mm) are shown on the right-hand side of Fig. 3, from which it can be seen that the enlargement of the lasing beam size with increasing y is significant. This is due to the fact that the length of the gain medium created by a 226 nm laser becomes shorter for larger y, i.e., closer to the flame tip; the lasing beam divergence inversely depends on the gain medium length [19], and it turns out that the lasing beam divergence increases with y.

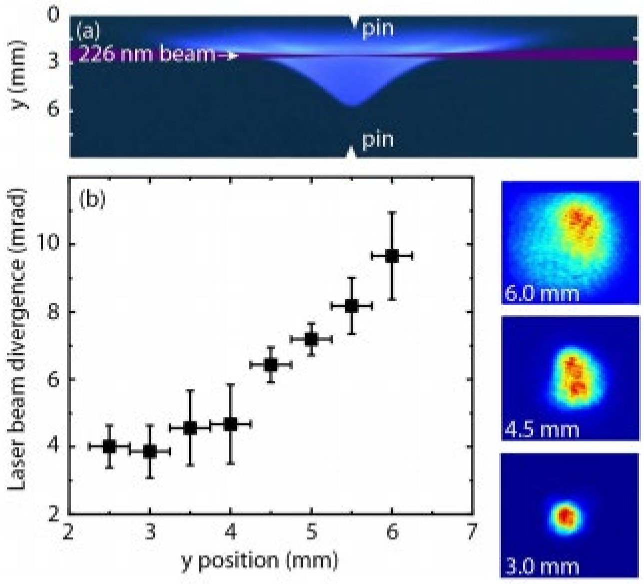

Fig. 3 *(a) Schematic illustration of focusing a 226 nm laser into the flame at different y positions. (b) Beam divergence of the backward 845 nm lasing as a function of y. The lasing beam images with 12 mrad × 12 mrad size taken by the iCCD camera for y = 3.0, 4.5, and 6.0 mm are also shown in the insets, respectively.*

It is notable in Fig. 1 that the flame is pushed down to the bottom electrode under NRP discharge-induced plasma forcing. Two-dimensional fs-TALIF imaging of atomic oxygen is conducted to measure its spatial distribution in the flame without and with plasma forcing. The results are shown in Fig. 4(a) and Fig. 4(b), respectively. The image shown in Fig. 4(b) is recorded ~1 μs after the discharge event. In addition to the push-down of the O-atom distribution, the fluorescence signal is enhanced significantly by the discharge forcing at the flame tip and in the vicinity of the flame front. Hence, the plasma forcing implies enhanced production of O atoms in the reaction zone of the flame. In addition, a faint fluorescence signal is noticeable in the discharge channel connecting the flame tip and the anode, which could come from atomic oxygen produced by plasma and post-discharge chemical reactions. In order to compare the fluorescence signals with the corresponding backward lasing signals, the fluorescence signal in the fs-TALIF image is integrated along the propagation direction of the pump laser and then plotted as a function of the vertical positions, as shown in Figs. 4(c) and 4(d).

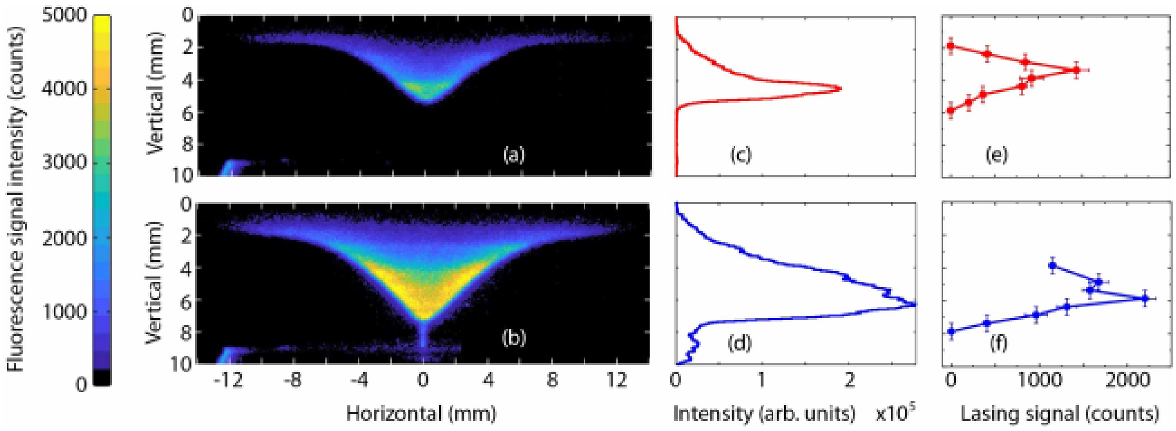

Fig. 4 *2D fs-TALIF images of atomic oxygen in (a) the base flame (without plasma) and (b) the flame under the glow discharge forcing (with plasma) (10 kHz repetition rate, 8.0 kV voltage). (c) and (d) Integrated fluorescence profiles of these two fluorescence images over the vertical direction, respectively. (e) and (f) Backward 845 nm lasing signal of atomic oxygen measured at different heights in the base flame and in the flame under the glow discharge forcing, respectively. The 226 nm laser pulse energy used in these measurements is ~100 μJ.*

To investigate the impact of plasma forcing on the flame using the BLT, the 226 nm pump laser has been focused at different heights in the flame, whereupon the backward lasing signal yield has been measured without and with plasma forcing. The results are shown in Figs. 4(e) and 4(f). The maximal backward lasing signal increased by ~54% during plasma forcing compared to the corresponding signal intensity in the unperturbed flame. This result agrees with the vertical profiles of the integrated fluorescence shown in Figs. 4(c) and 4(d). A slight vertical peak shift of the lasing signal can be noticed as compared with the integrated fluorescence peak, which is due to the increased length of the gain medium with shorter vertical distances. The maximal fluorescence signal exhibits a ~58% increase with plasma forcing. Similar percentages of increase between the fluorescence and backward lasing signals strongly indicate that these two methods have similar concentration dependence. This is because the backward lasing effect is close to the saturation regime of its optical gain with a maximum 226 nm pulse energy of ~100 μJ. An even closer agreement is expected with even higher 226 nm pulse energies.

To summarize, we generated bidirectional 845 nm lasing emission of atomic oxygen by focusing fs 226 nm laser pulses into a V-shaped lean methane-air flame. Particular focus was put on the backward lasing signal due to its potential applications for standoff remote sensing. To establish the presence of lasing, the lasing beam profile, divergence, and pump pulse energy dependence of the backward lasing were measured. The impact of NRP glow discharge forcing on the backward lasing strength was also investigated, and it was found to significantly enhance the signal strength by ~54%. By comparing the results from backward lasing with 2D fs-TALIF images of atomic oxygen, it was found that the vertical concentration profile can be reliably measured by the BLT. In the near-saturation regime, backward lasing shows similar concentration dependence as laser-induced fluorescence. These results suggest that the BLT could be a useful diagnostic tool for PAC studies, particularly in measurement geometries requiring single-ended standoff measurements.

Funding

Knut och Alice Wallenbergs Stiftelse; H2020 European Research Council; Stiftelsen för Strategisk Forskning; Vetenskapsrådet; Swedish Energy Agency through the Centre for Combustion Science and Technology; King Abdullah University of Science and Technology (BAS/1/1396-01-01).

Disclosures

The authors declare no conflicts of interest.

References

1. Q. Luo, W. Liu, and S. Chin, Appl. Phys. B 76, 337 (2003).

2. A. Dogariu, J. B. Michael, M. O. Scully, and R. B. Miles, Science 331, 442 (2011).

3. P. R. Hemmer, R. B. Miles, P. Polynkin, T. Siebert, A. V. Sokolov, P. Sprangle, and M. O. Scully, Proc. Natl. Acad. Sci. USA 108, 3130 (2011).

4. A. J. Traverso, R. Sanchez-Gonzalez, L. Yuan, K. Wang, D. V. Voronine, A. M. Zheltikov, Y. Rostovtsev, V. A. Sautenkov, A. V. Sokolov, S. W. North, and M. O. Scully, Proc. Natl. Acad. Sci. USA 109, 15185 (2012).

5. A. Laurain, M. Scheller, and P. Polynkin, Phys. Rev. Lett. 113, 253901 (2014).

6. S. Mitryukovskiy, Y. Liu, P. Ding, A. Houard, and A. Mysyrowicz, Opt. Express 22, 12750 (2014).

7. P. Ding, S. Mitryukovskiy, A. Houard, E. Oliva, A. Couairon, A. Mysyrowicz, and Y. Liu, Opt. Express 22, 29964 (2014).

8. P. N. Malevich, R. Maurer, D. Kartashov, S. Ališauskas, A. A. Lanin, A. M. Zheltikov, M. Marangoni, G. Cerullo, A. Baltuška, and A. Pugžlys, Opt. Lett. 40, 2469 (2015).

9. A. Dogariu and R. B. Miles, Opt. Express 24, A544 (2016).

10. P. Polynkin and Y. Cheng, Air Lasing (Springer, 2018), Vol. 208.

11. M. Aldén, U. Westblom, and J. E. M. Goldsmith, Opt. Lett. 14, 305 (1989).

12. J. E. M. Goldsmith, J. Opt. Soc. Am. B 6, 1979 (1989).

13. U. Westblom, S. Agrup, M. Aldén, H. M. Hertz, and J. E. M. Goldsmith, Appl. Phys. B 50, 487 (1990).

14. P. Ding, M. Ruchkina, Y. Liu, M. Alden, and J. Bood, Opt. Lett. 43, 1183 (2018).

15. P. Ding, M. Ruchkina, Y. Liu, M. Alden, and J. Bood, Opt. Lett. 44, 2374 (2019).

16. M. Ruchkina, P. Ding, A. Ehn, M. Aldén, and J. Bood, Proc. Combust. Inst. 37, 1281 (2019).

17. C. K. Law, Combustion Physics (Cambridge University, 2006).

18. S. Heitz, "Interaction mechanisms between nanosecond repetitively pulsed plasma discharges and laminar reactive flows," Ph.D. thesis (Université Paris-Saclay; Technische Universität, 2017).

19. G. I. Peters and L. Allen, J. Phys. A 5, 546 (1972).